A Nonredundant Multicolor Bar Code as a Screening Tool for Rearrangements in Neoplasia

Stefan Müller,[1] Verena Eder,[1] and Johannes Wienberg[1,2]*

[1]Institute of Anthropology and Human Genetics, Department of Biology II, Ludwig-Maximilians-University, Munich, Germany
[2]Institute of Human Genetics, GSF—National Research Center for Environment and Health, Munich, Germany

A chromosome bar code describes the colored pattern of chromosome segments and is derived by multicolor fluorescence in situ hybridization (FISH) of defined molecular probes. Published approaches to the simultaneous differentiation of whole karyotypes with bar codes have not allowed the unequivocal identification of all chromosome segments because of color redundancy of the patterns from a multitude of identically colored segments. Here, we present a chromosome bar code approach in which the problem of color redundancy has been overcome. It allows the detailed description of translocations, including breakpoints as well as intrachromosomal rearrangements in the karyotype of tumor cells. The resolution of discernable bars was increased to 100 bars per haploid chromosome set by including human chromosome–specific probes and more well-defined subregional probes such as chromosome arm- and segment-specific probes. Technically, no limitation to further increase in the resolution of the pattern became apparent. The approach was validated by the analysis of four established tumor cell lines widely used as models in cell biology, revealing numerous inter- and intrachromosomal rearrangements. Chromosome bar coding as presented here may provide further useful information for the subregional assignment of chromosomal breakpoints in complex chromosome aberrations, as found in various neoplasms that cannot be obtained by chromosome painting or classical banding techniques alone.

INTRODUCTION

The introduction of color codes on chromosomes by multicolor fluorescence in situ hybridization (FISH) of labeled DNA probes has added significantly to the definition of aberrant karyotypes. Chromosome-specific painting probes have been used to delineate the entire human karyotype in 24 distinct colors (Schröck et al., 1996; Speicher et al., 1996). Especially for tumor cytogenetics, multicolor painting approaches have strikingly demonstrated the value of molecularly defined probes in cases in which chromosome banding analysis alone failed to interpret the complex changes of entire karyotypes (Veldman et al., 1997; Ried et al., 1998; Fauth and Speicher, 2001).

Chromosome painting, however, only allows the identification of whole chromosomes and therefore is limited to the analysis of chromosome translocations. The delineation of intrachromosomal rearrangements (inversions, duplications, transpositions, gene amplifications, etc.) requires classical chromosome banding or the use of subregional DNA probes. A technique called chromosomal bar coding, which defines multiple chromosomes and chromosome segments by molecular probes (Lengauer et al., 1993), was introduced so that chromosomes and chromosome bands could be identified by their DNA content rather than their gray-scale banding patterns, as was done in classical cytogenetics (see Wienberg and Müller, 2002, for review). Reports in the literature have described subchromosomal probes that colorized chromosome segments such as YACs, cosmids, "fragmented hybrids," microdissection probes, chromosome-specific probes derived from species with evolutionarily fragmented karyotypes, and combinations thereof (Ried et al., 1992; Lengauer et al., 1993; Müller et al., 1997, 1998; Chudoba et al., 1999; Liehr et al., 2002). Application of such probes in a multicolor format results in a colored banding pattern of chromosomes, a chromosome bar code.

We recently introduced two strategies to colorize chromosome segments within entire karyotypes that also would enable us to screen for intrachromosomal rearrangements. Because the karyotypes of gibbons (hominoid primates) are highly fragmented by translocations, painting probes derived from these species can serve to delineate up to 90 chromosome segments in the

*Correspondence to: Johannes Wienberg, Institute of Anthropology and Human Genetics, Department Biology II, Ludwig-Maximilians-University, Richard-Wagner-Strasse 10, D-80333 Munich, Germany. E-mail: J.Wienberg@lrz.uni-muenchen.de

Received 13 June 2003; Accepted 2 September 2003
DOI 10.1002/gcc.10301

human karyotype (cross-species color segmenting, or RxFISH; Müller et al., 1998). Another approach makes use of DNA extracted from fragmented human chromosomes in human/rodent somatic cell hybrids (Müller et al., 1997). By definition, a bar code should have a nonredundant pattern that would definitively allow the discrimination of each bar and thus the unequivocal identification of each chromosome segment. Until now, however, this requirement could only be fulfilled with bar codes for individual chromosomes. In both previous approaches that aimed at the simultaneous differentiation of whole karyotypes (Müller et al., 1997, 1998), the definitive identification of each chromosome segment was hampered by color redundancy of the patterns as a result of a multitude of identically colored segments and thus did not represent a true bar code. To achieve proof of principle, we used only two fluorophores to differentially label DNA probes derived from fragmented chromosomes from human/rodent somatic cell hybrids (Müller et al., 1997). Recently however, experiments have been described using up to seven different fluorochromes in a single experiment (Saracoglu et al., 2001). The number of "tags" that can be set may be enhanced even more by sequential hybridization of different probes to the same metaphase spread (reFISH; Müller et al., 2002). Thus, the problem of color redundancy can be reduced by having probes labeled with more fluorochromes. Further, currently used bar code probes can be complemented with additional tags such that current probes would define chromosome segments not yet differentiated.

Here, we propose a true chromosome bar code. Composed of a set of human whole-chromosome painting (WCP) probes, probes specific for chromosome arms and segments, and yeast artificial chromosomes (YACs), it has improved banding resolution, yet avoids color redundancy. Using reFISH, we did two hybridizations of three- and four-probe pools each that implemented a total of seven image planes of the same metaphase cell and finally discriminated 100 regions of the human karyotype in a distinct, nonredundant color code. To test this approach, the set of probes was used for a detailed karyotype analysis of four tumor cell lines widely used in experimental biology: the melanoma cell line Mel Juso; two colon carcinoma cell lines, SW480 and SW620; and the T-cell lymphoma cell line Jurkat.

MATERIALS AND METHODS

Cell Samples, Cell Culture, and Metaphase Preparation

Metaphase spreads for in situ hybridization experiments were prepared from phytohaemagglutinin-stimulated peripheral lymphocytes of a normal human male as well as from the established tumor cell lines Jurkat (ATCC no. TIB-152, acute lymphoblastic T-cell leukemia; Schneider et al., 1977), Mel Juso (primary melanoma; Johnson et al., 1981), SW480 and SW620 (ATCC nos. CCL-228 and CCL-227, a colon cancer and metastasis from the same patient; Leibovitz et al., 1976). The cell line Mel Juso was kindly provided by Dr. J. Johnson, Institute for Immunology, Munich University. Cell culture and metaphase preparation followed standard procedures.

Multiplex Probe Composition

Two multiplex probe sets were designed for use in the hybridizations. The chromosome bar code (CBC) probe included all subregional probes and was color-labeled using three colors. To have unequivocal identification of all chromosome segments, the same metaphase cell was then hybridized with human WCP probes, which were labeled with four different fluorochromes.

Subregional probes were mainly derived from nonhuman primates with evolutionarily fragmented karyotypes. The entire set of WCP probes from gibbons (Müller et al., 1998) was used and supplemented with a few probes derived from African green monkeys (Finelli et al., 1999) and tamarins (Müller et al., 2001). The African green monkey probes delineated human homologous chromosome segments 2q13-qter and 4q, whereas the tamarin probes hybridized to the human homologous chromosome segment 1q32-qter.

The bar code probe was further supplemented by a YAC (860_g_08, specific for 21q22.3), fragmented hybrids 377 and 304 (segments 2q35-qter, Xp11.2, and 5q34-qter; Antonacci et al., 1995), and microdissected probes specific for entire chromosome arms (1p, 2p, 3p, 7p, 9p, 11p, 16p, 17p, 18p, 19p, and Xq; Guan et al., 1996) or individual bands (6qter, 8qter, 11qter, 13qter, 15qter, 16qter, 18qter, 22qter, Xpter, and Yqter; Fauth et al., 2001). The YAC was obtained from the DHGP Resource Centre (Berlin, Germany). The fragmented hybrids were kindly provided by Dr. M. Rocchi, Bari University (Bari, Italy). Some of the microdissected probes were purchased from Research Genetics (Huntsville, AL, USA), and the others were generous gifts from Dr. M. Speicher (Technical Univer-

sity Munich, Munich, Germany) and Dr. J. Trent (National Cancer Institute, Bethesda, MD, USA). The human DNA content of fragmented hybrids was enriched by Alu-PCR, as described by Antonacci et al. (1995). Degenerate primers were then used to transfer these Alu-PCR products into degenerate oligonucleotide–primed polymerase chain reaction (DOP-PCR) products (Telenius et al., 1992). All other DNA probes were directly amplified by DOP-PCR. The bar code probes were divided into three subsets (CBC 1–3), each of which was labeled with a different fluorochrome. The complementary human WCP probe set comprised four subsets, each of which was labeled with a different fluorochrome (Fig. 1A).

Probe Labeling

An adapted version of the protocol introduced by Roberts et al. (1999) guided the composition of the two multiplex probes. This protocol includes constructing probe pools for each of the seven subsets. Thus, from each "member" of a subset, either 100–200 ng of WCP or 200–500 ng of DNA (YACs, fragmented hybrids, microdissected probes), depending on the quality of the individual probes, was pooled. Each subset was reamplified by DOP-PCR, using 150 ng of the pooled template DNA. In a further round of DOP-PCR, each probe subset was labeled with fluorochrome or hapten-conjugated 2′-deoxyuridine 5′-triphosphate (dUTP). The probe labeling scheme was as follows: CBC probe subsets were labeled with biotin-dUTP (Roche), digoxigenin-dUTP (Roche), and TAMRA-dUTP (Perkin Elmer). The WCP probe subsets were labeled with biotin-dUTP, digoxigenin-dUTP, dinitrophenol-dUTP (Perkin Elmer), and TAMRA-dUTP. Mixed with 2.5 μg of each of the CBC and WCP sets were 10 μg of human Cot-1 DNA, ethanol-precipitated and resuspended in hybridization buffer (50% formamide, 1× SSC, 10% dextrane sulfate).

Sequential Hybridization In Situ and Probe Detection

Both probe sets were sequentially hybridized to the same specimen, according to the reFISH protocol (Müller et al., 2002). The CBC probe was hybridized first. It was denatured at 70°C for 7 min and preannealed by incubation at 37°C for 30 min. The chromosomes on slides were denatured in 70% formamide/2× SSC at 72°C for 1.5 min. The hybridization was carried out for 48 hr, followed by serial washings as follows: twice in 50% formamide/2× SSC at 45°C for 5 min each time; twice in 2× SSC at 45°C for 5 min each time; and once in 0.1× SSC at 60°C for 5 min. Biotinylated DNA probes were detected by avidin–Cy5 (Amersham), digoxigenin-labeled probes by sheep antidigoxigenin fluorescein-isothiocyanate (FITC)–conjugated antibody (Roche). Before rehybridization with the WCP probe set, the coverslip and the antifading solution were removed from the slide by soaking it in 4× SSC/0.2% Tween. This was followed by serial ethanol dehydration (70%, 90%, 100%), fixation in methanol/acetic acid (3:1 v/v) for 30 min at room temperature, and incubation overnight at 37°C. The slide denaturation time was extended to 2.5 min. The stringency washes done were identical to those after the first hybridization. The WCP probe set was detected by avidin-AMCA (7-amino-4-methylcoumarin-3-acetic acid), sheep antidigoxigenin Cy5–conjugated antibody (Roche), and goat antidinitrophenol/rabbit antigoat FITC (both Sigma).

Microscopic Setup and Image Analysis

After each of the two hybridizations, metaphase cells were visualized with a cooled CCD camera (Photometrics NU200 equipped with a KAF1400 chip) coupled to a Zeiss Axiophot microscope. Blue (DAPI counterstain), green, red, and infrared fluorescence were analyzed through a quadruple filter set, and a single-band-pass filter was used for AMCA (all from Chroma Technology, Brattleboro, VT). The cell coordinates on the slide were recorded by an automated XY motorized stage (Ludl), which allowed cell repositioning after the second hybridization. The CCD camera and stage were controlled by SmartCapture Viewpoint software (Digital Scientific, Cambridge, UK).

RESULTS

Hybridization to Diploid Human Lymphocyte Metaphase Preparations

The present CBC probe yielded 100 segments on normal diploid human chromosomes per haploid set in seven colors derived from the combination of three fluorochromes. In each color combination, 12–15 bars were stained (Fig. 1A). The WCP probe set labeled with four fluorochromes yielded 15 color combinations. The labeling scheme was chosen so that each chromosome tagged with bars of identical color in the CBC probe would be labeled with a different fluorochrome combination with the WCP probe set. For example, yellow segments on chromosomes 1, 2, 4, 9, 11, 12, 14, 15, 17, 18, and 19 were stained in different colors with WCPs. On the

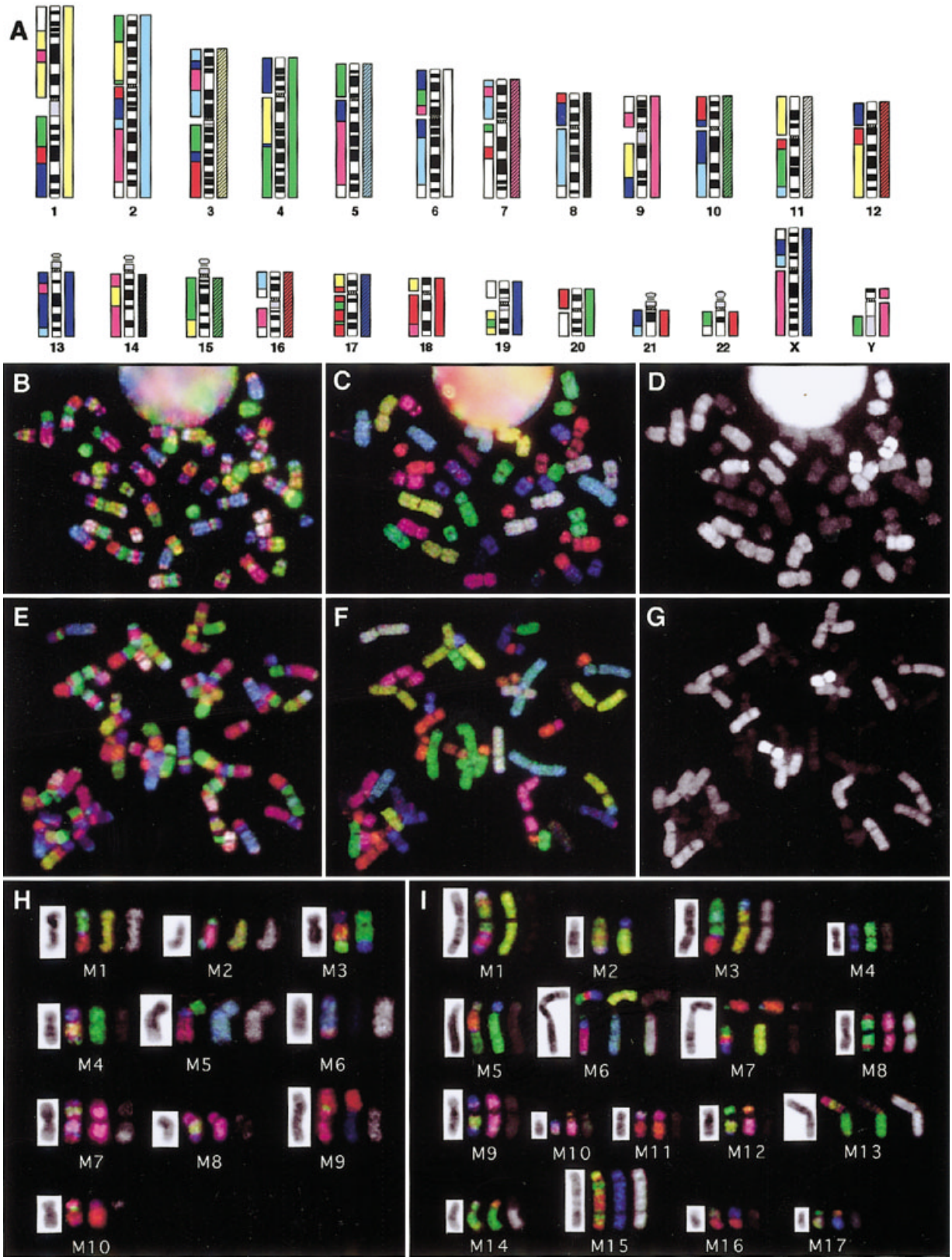
A
1
2
3
4
5
6
7
8
9
10
11
12
13
14
15
16
17
18
19
20
21
22
X
Y
B
C
D
E
F
G
H
M1
M2
M3
M4
M5
M6
M7
M8
M9
M10
I
M1
M2
M3
M4
M5
M6
M7
M8
M9
M10
M11
M12
M13
M14
M15
M16
M17

Figure 1.

TABLE 1. Numerical and Structural Aberrations Observed in Cell Line Jurkat (Acute Lymphoblastic T-Cell Leukemia)

Numerical abnormalities		Cells 1–10									
3		2	2	2	1	2	2	2	2	2	2
4		1	1	1	1	1	1	2	1	1	2
8		1	1	1	1	1	1	1	1	1	1
9		0	0	0	0	0	0	0	0	0	0
18		1	1	1	1	1	1	1	1	1	1
20		2	3	2	2	3	3	3	3	3	2
Y		0	0	0	0	0	0	0	0	0	0
Structural rearrangements											
M1	del(3)(pter→p13)			X	X						
M2	del(3)(p13→qter)			X	X						
M3	der(4)t(4;19)(q27;q12)			X							
M4	del(4)(q27)	X	X		X	X	X		X	X	
M5	del(5)(q35)		X	X			X	X	X	X	X
M6	del(8)(p11)	X	X	X	X	X	X	X	X	X	X
M7	der(9)t(8;9)(p11;p21)	X	X	X	X	X	X	X	X	X	X
M8	del(9)(p21)	X	X	X	X	X	X	X	X	X	X
M9	der(18)t(X;18)(q11;p11.2)	X	X		X	X	X	X	X	X	X
M10	der(18)t(X;18)(q11;p11.2)del(X)(q12)			X							

other hand, chromosomes 4 and 20 were assigned the same WCP probe label because these chromosomes did not share any segments of identical CBC color. In total, each segment was tagged with a unique combination of the three plus four fluorochromes/haptens (Fig. 1A). The chromosomal counterstain (DAPI) provided supplementary banding information, which was particularly informative for the determination of chromosomal boundaries. The hybridization patterns demonstrated that the origin of each segment could clearly be distinguished. No redundant color pattern was observed in any of the 100 chromosome segments.

Figure 1. (A) Ideogrammatic illustration of the hybridization pattern on normal human chromosomes obtained with the combined probe sets CBC and WBC, resulting in a nonredundant chromosome bar code. To the left of each chromosome, the CBC probe hybridization pattern is shown as RGB display: probes detected with FITC are shown in green, TAMRA-labeled probes in red, probes detected with Cy5 in blue, and probes with more than one fluorochrome in the respective mixed colors. The color code corresponds to that found in the tumor sample metaphases displayed in Figures 1B and E and 2A. To the right of each chromosome ideogram, the WCP probe pattern is illustrated. Human painting probes detected with FITC are shown in green, TAMRA-labeled probes in red, probes detected with Cy5 in blue, and probes detected with more than one fluorochrome in the respective mixed colors (corresponding to tumor metaphase images in Figs. 1C and F and 2B). Chromosomes detected with AMCA are hatched and displayed separately in tumor metaphase images in Figures 1D and G and 2C. (B)–(D) Illustrations of representative metaphases of the acute lymphoblastic T-cell leukemia cell line Jurkat. (E)–(G) Metaphase of the primary melanoma cell line Mel Juso. All marker chromosomes observed in these two cell lines are summarized in Figure 1H (Jurkat) and I (Mel Juso). For each marker chromosome (from left to right): inverted counterstain (DAPI), CBC (FITC/TAMRA/Cy5), WCB (FITC/TAMRA/Cy5), and WCP (AMCA) pattern.

Bar Code Analysis of Tumor Cell Lines

To validate the feasibility of this approach, four samples from established tumor cell lines were analyzed. After sequential hybridization of both the CBC and WCP probe sets, 10 metaphase cells from the cell line Jurkat were fully analyzed by visual inspection of the obtained hybridization pattern. Figure 1B–D displays representative hybridization images. The results revealed a rather uniform pseudodiploid karyotype of $2n = 45–48$ with approximately 10% tetraploidy. Table 1 summarizes the chromosomal aberrations observed. Numerical abnormalities involved chromosomes 3, 4, 8, 9, 18, 20, and Y. In total, 10 marker chromosomes were noticed, 6 of them occurring in more than 70% of the cells analyzed (Fig. 1H, Table 1). The karyotype appeared balanced, except for underrepresented chromosomes and chromosome regions 4q27→qter, 9, 18q11→pter, 20, and Y and overrepresented chromosomes 5pter→q34 and Xq.

Fifteen cells of the female melanoma cell line Mel Juso were completely analyzed after sequential hybridization of the CBC and WCB probe sets. Figure 1E–G illustrates the results for a representative cell. The chromosome number in this near-diploid cell line varied between 44 and 47. Chromosomes 2, 6, 8, 10–13, 16, 21, and X were found to be in a diploid state; all other chromosomes were involved in structural or numerical abnormalities (Table 2). Seventeen marker chromosomes were observed, as illustrated in Figure 1I. This cell line comprises two subclones, which can be distinguished by markers M5 and M17. M4 and M11

TABLE 2. Numerical and Structural Aberrations Observed in Cell Line Mel Juso (Primary Melanoma)

		Cells 1–15														
Numerical abnormalities		Clone 1								Clone 2						
1		1	1	0	1	1	1	1	1	1	1	1	1	1	1	1
4		1	1	1	2	1	1	2	1	2	1	2	2	2	2	2
5		1	1	1	1	1	1	0	1	1	1	1	1	1	1	1
7		2	2	2	2	1	1	2	1	2	2	2	2	2	2	2
9		0	0	0	1	0	0	0	0	0	1	0	0	0	0	0
14		1	1	1	1	1	1	1	1	1	1	1	1	1	1	1
15		0	0	0	0	0	0	0	0	0	0	0	0	0	0	0
17		1	1	1	1	1	1	1	1	1	1	1	1	1	1	1
18		1	1	1	1	1	1	1	1	2	1	2	2	2	1	2
19		1	1	1	1	1	1	1	1	1	1	1	1	1	1	1
20		3	3	2	3	3	3	3	2	3	3	3	3	3	3	2
22		1	1	1	1	1	1	1	1	1	1	1	1	1	1	1
Structural rearrangements																
M1	inv(1)(q31q41)			X												
M2	der(1;19)(p11;q11)	X	X	X	X	X	X	X	X	X	X	X	X	X	X	X
M3	der(3)t(3;5)(p14;p13)	X	X	X	X	X	X	X	X	X	X	X	X	X		X
M4	i(4)(p11)	X	X	X		X	X		X		X					
M5	der(4;19)(q11;p11)	X	X	X		X	X		X							
M6	der(5)t(1;5)(q12;p13)	X	X		X	X	X	X	X	X	X	X	X	X	X	X
M7	der(5)t(1;5;18)(q12;p13;q12)			X												
M8	i(7)(p11)	X	X	X	X	X	X	X		X	X	X	X	X	X	X
M9	del(9)(p21)	X	X	X	X	X	X	X	X	X	X	X	X	X	X	X
M10	del(9)(q12)	X	X	X	X	X	X	X	X	X	X	X	X	X	X	X
M11	der(9;18)(p11;p11)	X	X	X	X	X	X	X	X		X				X	
M12	der(9;22)(q11;q11)del(22)(q13)	X	X		X	X	X	X	X	X	X	X	X	X	X	X
M13	der(14;15)(q11;q11)	X	X	X	X	X	X	X	X	X	X	X	X	X	X	X
M14	der(15;22)(q11;q11)	X	X	X	X	X	X	X	X	X	X	X	X	X	X	X
M15	der(17)t(17;17;17)(q?;q?;q11)	X	X	X	X	X	X	X	X	X	X	X	X	X	X	X
M16	der(18;19)(q11;p11)				X			X								
M17	der(19)t(19;22)(p11;q?)									X	X	X	X	X	X	X

were preferentially found together with M5 (clone 1). M16, which may be derived from M11, was found only in two cells. M7 most probably is a derivative of M6, and, like M1, it was found only in a single cell. Chromosomes and chromosome regions 3p14→pter, 4p (clone 1), 7p, 17q, and 20 were present in three copies, whereas chromosome regions 9p21→pter and 18q were found only in a single copy (clone 1).

In our study, the cell line SW480 showed a hyperdiploid karyotype, with the chromosome number varying between 50 and 55 (Fig. 2). In the 15 cells analyzed, only chromosomes 4, 6, 10, 14–16, and 20 were not involved in any structural or numerical abnormalities. In contrast to the results of a recent study by spectral karyotyping (SKY) by Melcher et al. (2000), 28 marker chromosomes were detected (Table 3, Fig. 2D), compared to the 13 found in the previous SKY analysis. All derived chromosomes found in both studies were in good agreement. For six marker chromosomes, however, different breakpoints were detected. In two additional markers, the chromosome bar code probe provided additional subregional definition: Marker der(8)t(8;9) was identified as M21, der(9)t(8;9)(q12;p13) and marker der(19)t(19;8;19;5) as M27, der(19)t(19;8;19;5)(p?;q?;q?;p?), respectively. Genomic imbalances were found in the following regions: overrepresentation of 2pter→q24, 7pter→q22, 8pter→p23, 8q, 10p15?→pter, 11, 12p, 13q14?, 17, 19p?, and X and deletion of 5q14→31, 9q, 12q11→13, 31q21→qter, 18q12→qter, and Y.

In cell line SW620, chromosome numbers varied between 47 and 52 (15 cells analyzed). All chromosomes except 9, 12, 17, 19, 21, and 22 were involved in numerical aberrations. In total, 36 marker chromosomes were observed, reflecting a highly complex karyotype. (Fig. 2A–C, E; Table 4). In five markers (M3, M12, M13, M18, and M21), different breakpoints were identified, compared to the recent SKY analysis of this cell line (Melcher et al., 2000). The presence of two distinct subclones (60% cl1, 40% cl2) with a distinct spectrum of derivative chromosomes was confirmed. Clone 2 exhibits a higher rate of genomic instability, with

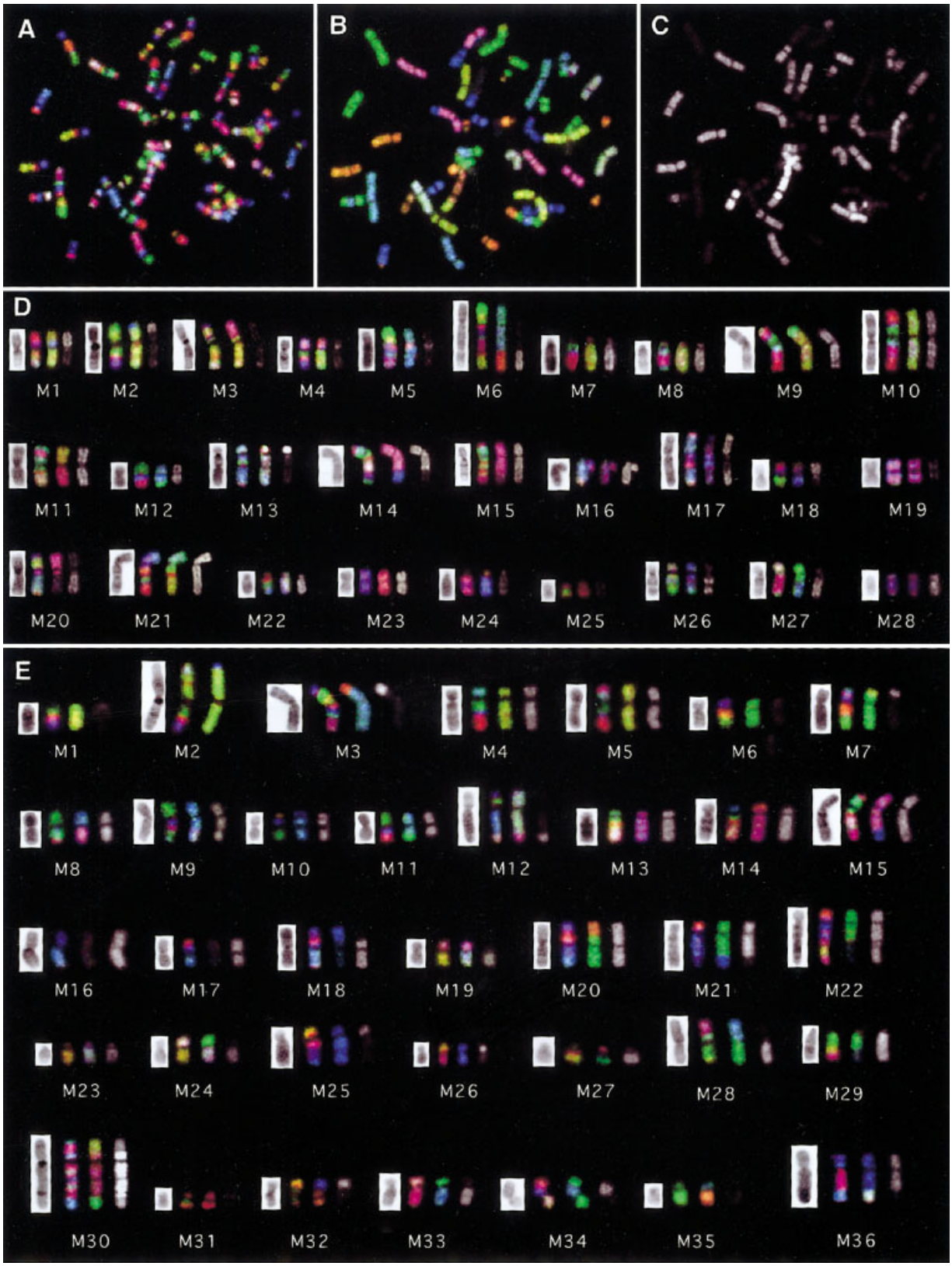

Figure 2. Bar code analysis of colon carcinoma cell lines SW 480 (primary tumor) and SW 620 (metastasis from the same patient). Refer to Figure 1A for the probe color code. Representative illustrations of SW 620 metaphases after hybridization shown for the (A) CBC and (B and C) WCB probes. All marker chromosomes observed in the two cell lines SW 480 and SW 620 are summarized in (D) and (E), respectively. For each marker chromosome (from left to right): inverted counterstain (DAPI), CBC (FITC/TAMRA/Cy5), WCB (FITC/TAMRA/Cy5), and WCP (AMCA) pattern.

TABLE 3. Numerical and Structural Aberrations Observed in Cell Line SW480 (Colon Cancer, Primary Tumor)

Numerical abnormalities		Cells 1–15														
1		0	1	1	1	1	1	1	1	1	1	1	1	1	1	1
2		2	1	2	2	1	2	2	2	2	2	2	2	2	2	2
3		1	1	1	1	0	1	1	1	1	1	1	1	1	1	1
5		1	1	1	1	1	1	1	1	1	1	1	1	1	1	1
7		2	2	2	2	1	2	2	2	2	2	2	2	2	2	2
8		0	0	0	1	0	1	0	0	0	0	0	0	0	0	0
9		1	1	1	1	1	0	1	1	1	1	1	1	1	1	1
11		3	2	3	3	3	3	3	3	3	3	3	3	3	3	3
12		1	1	1	1	1	1	1	1	1	1	1	1	1	1	1
13		1	1	1	2	1	2	1	1	1	1	1	1	1	1	2
17		3	3	3	3	3	2	3	3	3	3	3	3	3	3	3
18		1	1	1	1	1	1	1	1	1	1	1	1	1	1	1
19		1	1	1	1	1	1	1	1	1	1	1	1	1	1	1
21		2	2	2	2	2	2	3	2	2	2	3	3	2	2	2
X		1	1	2	1	0	2	2	2	2	2	1	2	2	1	2
Y		0	0	0	0	0	0	0	0	0	0	0	0	0	0	0
Structural rearrangements																
M1	der(1;3)t(1;3;5)(p21;q24;q13)	X														
M2	der(1)t(1;5)(p22;p?)	X														
M3	der(1)t(1;9)(q21;q12)	X	X	X	X	X	X	X	X	X	X	X	X	X	X	X
M4	der(1;9)(q12;p11)	X	X	X	X	X	X	X	X	X	X	X	X	X	X	X
M5	del(2)(q11.1q14.1)ins(2;7)(q11.1;q?)		X													
M6	der(2)t(2;12)(q24;q13)	X	X	X	X	X	X	X	X	X	X	X	X	X	X	X
M7	del(3)(p11)								X			X	X			
M8	del(3)(q11)	X	X	X	X		X	X	X	X	X	X	X	X	X	X
M9	der(3)t(3;20)(q31;q12)inv(3)(p21q31)	X		X		X										
M10	der(3)inv(p?24q26.3)del(3)s(p?24)				X		X	X		X				X	X	X
M11	der(3;7)(p11;q11)					X										
M12	der(5)t(5;20)(q14;p12)		X	X	X	X	X	X	X	X	X	X	X	X	X	X
M13	dic(6;16)(p25;p11)											X				
M14	der(7)t(7;13)(q32;q22)	X	X	X	X	X	X	X	X	X	X	X	X	X	X	X
M15	der(7)inv(7)(q22q36)t(7;14)(q22;q22)	X	X	X	X			X	X			X			X	
M16	del(8)(p23)	X	X	X	X	X	X	X	X	X	X	X	X	X	X	X
M17	i(8)(q11)ins(8;13)(p11;q?)	X	X	X				X	X	X	X	X	X		X	X
M18	der(8;19)(p11;q11)	X	X	X	X	X	X	X	X	X	X	X	X	X	X	X
M19	i(9)(p11)						X									X
M20	der(9)t(8;9)(q12;p13)					X	X									X
M21	der(10)t(3;10;12)(q13;p?15;q12)	X	X	X	X	X	X	X	X	X	X	X	X	X	X	X
M22	del(11)(p11)		X													
M23	i(12)(p11)	X	X	X	X	X	X	X	X	X	X	X	X	X	X	X
M24	der(13)invdup(13)(q14q?)del(13)(q21)	X	X	X	X	X	X	X	X	X	X	X	X	X	X	X
M25	del(18)(q12)	X	X	X	X	X	X	X	X	X	X	X	X	X	X	X
M26	der(19)t(19;8;19;5)(p?;q?;q?;p?)	X	X	X	X	X	X	X	X	X	X	X	X	X	X	X
M27	der(20)t(5;20)(q31;p12)	X	X	X	X	X	X	X	X	X	X	X	X	X	X	X
M28	i(X)(p11)														X	

12 marker chromosomes found in a minority of cells, compared to only one in clone 1. Both subclones also showed a different pattern of genomic imbalances. In subclone 1, chromosomes Y, 3, 4q28→qter, and 18q12→qter were deleted, and 5p, 7p, 7q32→qter, 12p, 13q21→qter, 16, 17p 18pter→q12, 20p, and 22 were overrepresented. Subclone 2 showed underrepresentation of chromosomes 3 and 18, whereas 8p, 11p, 12p, 13, 17p and 20p were present in more than two copies per cell. Marker chromosomes M11 (cl2), M31 (cl1), and M33 (cl1 and cl2) were present both in cell line SW 480 and in cell line SW 620.

DISCUSSION

Increasing the Resolution of Bar Code Probes

The present study provides for the first time a nonredundant multicolor chromosome bar code with multiple bars for each chromosome for the

TABLE 4. Numerical and Structural Aberrations Observed in Cell Line SW620
(Colon Cancer, Metastasis from the Same Patient Shown in Table 3)

		Cells 1–15														
Numerical abnormalities		Clone 1									Clone 2					
1		2	2	2	2	2	2	2	2	2	1	1	1	1	1	1
2		1	1	1	1	1	1	1	1	1	3	2	2	2	3	2
3		1	1	1	1	1	1	1	1	1	0	1	1	0	0	1
4		2	2	1	1	2	2	2	2	2	2	2	2	2	2	1
5		1	1	1	1	1	1	1	1	1	1	1	1	1	1	1
6		1	1	1	1	1	1	0	1	1	2	2	2	2	2	2
7		2	2	2	2	2	2	2	2	2	2	3	2	3	3	2
8		1	0	0	1	1	1	1	1	1	1	1	0	1	1	1
10		1	1	1	1	1	1	1	1	1	1	1	1	1	1	1
11		3	3	3	3	3	2	3	3	3	2	2	2	2	2	2
13		2	2	2	2	2	2	2	2	2	1	1	2	1	1	1
14		2	2	2	2	2	2	2	2	2	0	0	0	0	0	0
15		2	2	2	1	2	2	2	2	2	1	1	1	1	1	1
16		1	1	1	1	1	1	1	1	1	1	1	1	1	1	1
18		1	1	1	1	1	1	1	1	1	1	1	1	1	1	1
20		2	2	2	2	2	2	2	2	2	2	2	1	1	2	1
X		1	1	1	1	1	1	1	1	1	2	2	1	2	2	2
Y		0	0	0	0	0	0	0	0	0	0	0	0	0	0	0
Structural rearrangements																
M 1	del(1)(p11)					X		X								
M 2	der(1)t(1;19)(p36.3;p13.2)														X	
M 3	der(2)t(2;12)(p24;p12)	X	X	X	X	X	X	X	X	X						
M 4	del(3)(p14)	X	X	X	X	X	X	X	X	X	X	X	X	X	X	X
M 5	del(3)(p21)										X			X	X	
M 6	del(4)(q28)	X	X	X	X	X	X	X	X	X						
M 7	der(4)t(3;4)(p21;p16)										X	X	X	X	X	X
M 8	der(5;7)(p11;p11)	X	X	X	X	X	X	X	X	X						
M 9	der(5)t(5;11)(q21;q22)														X	
M 10	der(5)t(5;17)(q13;p12)	X	X	X	X		X		X	X						
M 11	der(5)t(5;20)(q15;p12)										X	X	X	X		X
M 12	der(6)t(6;7)(q23?;q32)	X	X	X	X	X	X	X	X	X						
M 13	del(7)(p13)										X				X	
M 14	der(7)t(7;21)(p13;q22?)															X
M 15	der(7)t(7;X)(q32;q?)												X			
M 16	der(8)del(8)(p21)										X	X		X	X	X
M 17	der(8)del(8)(q13)												X			
M 18	der(8)t(8;13)(p23;q21)	X	X	X	X	X	X	X	X	X	X	X	X	X	X	X
M 19	der(9;11)(p11;q11)															X
M 20	der(10)t(10;12)(p15;p11)										X	X	X	X	X	X
M 21	der(10)t(10;13)(q22;q?)	X	X	X	X	X	X	X	X	X						
M 22	der(10)t(10;14)(q22;q11)										X	X	X	X	X	X
M 23	del(11)(q11)												X			
M 24	der(11;20)(p11;q11)													X		X
M 25	der(13;17)(q11;p11)											X				
M 26	der(13;17)(q11;p11)del(13)(q14)										X	X	X	X	X	X
M 27	der(14)t(14;15)										X	X	X	X	X	X
M 28	der(15)t(2;15)(q21;q11)											X				
M 29	der(15)t(14;15)(q13;q?)										X		X	X	X	X
M 30	der(16)t(3;16;8;16;10)(p21;p13;p?;q12?;q22)	X	X	X	X	X	X	X	X	X	X	X	X	X	X	X
M 31	del(18)(q12)	X	X	X	X	X	X	X	X	X						
M 32	der(18)t(17;18)(p11.2;q12)	X	X	X	X		X		X	X						
M 33	der(20)t(5;20)(q13;p11.2)	X	X	X	X	X	X	X	X	X	X	X	X	X	X	X
M 34	ins(20;5)(p11.2;q11q13)												X	X		
M 35	der(22)t(2;22)(p23;q11)	X	X	X	X	X	X	X	X	X						
M 36	der(X)t(X;6)(q27?;q23?)	X	X	X	X	X	X	X	X	X						

differentiation of the entire human karyotype. This progress was made possible through advances both in fluorescence microscopy and in multicolor FISH procedures (Roberts et al., 1999; Schröck and Padilla-Nash, 2000; Fauth and Speicher, 2001; Müller et al., 2002). Currently, the only limitation of the strategy presented here is the expense of the probe labels and the workload in the construction of these complex probe sets. The expense of the probe labels, however, may be significantly reduced when fluorescent nucleotides are synthesized according to the principles outlined in Henegariu et al. (2000).

Several improvements have been made in this bar code compared to previous chromosome bar code strategies for differentiating the entire human karyotype (Müller et al., 1997, 1998). First, the banding resolution was increased to 100 bars per haploid chromosome set. Each chromosome was subregionally defined by at least two (chromosome 22) and up to seven bars (chromosome 2). This was achieved by including various well-defined subregional probes derived from nonhuman primate species, rearranged somatic cell hybrid cell lines, and microdissected human chromosome segments, as well as a YAC clone. More important, the complementation with human paint probes provided a way to overcome the problem of color pattern redundancy, inherent in previous whole-karyotype bar code approaches. Each bar can now be unequivocally assigned to a defined human chromosome region, and the identification of chromosomal material is not hampered any more by a multitude of segments of the same color. In total, the present bar code probe set is equivalent to a multiplex probe set composed of 100 individual combinatorially labeled subregional probes and therefore provides superior subregional definition compared to the to-date most complex multiplex probe set that would simultaneously define all human chromosome arms (Wiegant et al., 2000). Thus, this approach may present an advance over current M-FISH or SKY strategies, because it combines reproducible color karyotyping for the detection of chromosomal material in translocations with a detailed definition of chromosome subregions.

We used reFISH to demonstrate that this number of segments can even be differentiated on microscopes with a "conservative" setup using conventional band-pass filters (Müller et al., 2002). For this purpose, the CBC probe set was labeled with three fluors yielding seven color combinations. It was hybridized first and was detected together with the chromosomal counterstain DAPI. It was designed to produce bars of identical color on 15 or fewer different chromosomes. The resulting color redundancy was overcome with the second hybridization of the four complementary WCP probe sets. The WCP probe set yielded 15 color combinations and was composed in a way to differentially stain those chromosomes previously tagged with bars of identical color. Therefore, the present microscopic setup limited the number of segments (S) to be unequivocally discriminated to $7 \times 15 = 105$ ($S = NM$, where N and M are the numbers of the CBC and WCP color combinations, respectively). In a more advanced microscopic setup, the same number of uniquely labeled segments can of course be defined in a single hybridization by just using seven discernible fluorochromes.

Alternatively, given the possibility to simultaneously discern more fluorochromes with a dedicated microscopic setup, a human WCP probe set composed of purely combinatorially labeled probes with five fluorochromes may be applied. In this case, all human chromosomes could be readily identified with the WCP probe. Consequently, the number of bars produced by an additional CBC probe and therefore its resolution would theoretically be virtually unlimited. In reality, it would solely depend on the hybridization efficiency and the spatial resolution of individual subregional probes used in the CBC probe set.

Obviously, a way to realize the goal of increasing the number of bars beyond the resolution of classical banding techniques would be to include a large number of genetically well-defined BAC clones. This approach would also allow a direct link of chromosomal breakpoints to the human genome sequence. This strategy was recently tested by Liehr et al. (2002) for a generation of high-resolution chromosome bar codes for individual chromosomes. However, the authors concluded that the YAC- or BAC-based bar codes did not fulfill expectations in flexibility, hybridization efficiency, and resolution, compared to microdissection-derived band-specific painting probes. In our hands, a chromosome 7–specific bar code probe composed of 35 BAC clones obtained from the Human BAC Resource Consortium (http://www.ncbi.nih.gov/genome/cyto) was equally unsatisfying (our unpublished data). The complexity of BACs and the contamination with bacterial DNA may require a more efficient PCR amplification and labeling procedure of human vector cloned DNA than is currently available. The recent introduction of novel sets of dedicated DOP primers (Fiegler et al., 2003), which showed a sixfold increase in the amplification of human BAC

cloned DNA compared to conventional primers, will certainly be helpful.

Application of the Bar Code Probe to Tumor Cytogenetics

Our approach was validated by analysis of four established tumor cell lines widely used as models in cell biology. The aims were (1) to evaluate whether the chromosome bar coding presented in this study equals other multicolor FISH karyotyping studies in resolution and reproducibility and (2) to add additional information by better defining chromosome subregions.

The colon carcinoma cell lines SW 480 and SW 620 (Fig. 2) were chosen because they were previously investigated by SKY (Melcher et al., 2000). Compared to the results found in the previous SKY analysis, our study showed more than twice the number of marker chromosomes in SW 480, although all derivative chromosomes that were common to both studies were in good agreement. It cannot be ruled out that the differences in the number of rearranged chromosomes observed between this study and the previous SKY analysis are simply culture artifacts and the result of different evolutions of subclones of this cell line. For six marker chromosomes identified in the SKY analysis and the present work, however, different breakpoints were postulated from the bar code pattern. In two further markers, the chromosome bar code probe provided additional subregional definition. Compared to the results of the previous analysis of cell line SW 620 by SKY, our study identified an almost identical pattern of the remaining marker chromosomes by the nonredundant chromosome bar code probe and SKY.

In addition to the colon carcinoma cell lines, two well-known tumor cell lines, as yet uncharacterized by molecular cytogenetics, were analyzed with the bar code probe: the melanoma cell line Mel Juso and the acute lymphoblastic T-cell leukemia cell line Jurkat. In primary melanomas, chromosomes 1, 6, 7, 8, 9, 10, and 11 are frequently involved in numerical or structural aberrations (Thompson et al., 1995; Balazs et al., 2001; Schulten et al., 2002). Of these rearrangements, cell line Mel Juso showed gains of 7p, involving the *EGFR* gene, and loss of 9p21→pter, involving the *CDKN2A* tumor suppressor gene locus. Furthermore, various cases with an i(17q) have been described in primary melanomas (http://cgap.nci.nih.gov/chromosomes/Mitelman). Marker M15, a complex der(17)t(17;17;17)(q?;q?;q11) found in every cell, does contain two copies of 17q resembling an i(17q) but also contains additional 17pter→q? material. It also may be assumed from the hybridization pattern of the chromosome 17 WCP that M15 is dicentric.

Although the cell line Jurkat shows 10 marker chromosomes, none is characteristic for ALL, except for a deletion and a translocation involving the 9p21 region (M7 and M8, respectively) harboring the *CDKN2A* locus. Neither did we observe numerical aberrations involving chromosomes 4, 6, 10, 14, 17, 18, 21, or X (Harrison and Foroni, 2002).

We conclude that the present chromosome bar code approach allows a detailed description even of complex chromosome aberrations characteristic of various tumors. Translocations can be detected with at least the same confidence as in conventional M-FISH or SKY karyotyping studies. In addition, the bar code approach provides useful information for subregional assignment of chromosomal breakpoints that cannot be obtained by chromosome painting alone. Thus, this technique may span the bridge between chromosome painting for the identification of chromosome translocations and conventional banding analysis or FISH of defined clones for the assignment of the breakpoints involved. Probe sets such as those presented here will be made accessible to the cytogenetic community for additional evaluation of their resolution and efficiency in different areas of cancer cytogenetics.

REFERENCES

Antonacci R, Marzella R, Finelli P, Lonoce A, Forabosco A, Archidiacono N, Rocchi M. 1995. A panel of subchromosomal painting libraries representing over 300 regions of the human genome. Cytogenet Cell Genet 68:25–32.

Balazs M, Adam Z, Treszl A, Begany A, Hunyadi J, Adany R. 2001. Chromosomal imbalances in primary and metastatic melanomas revealed by comparative genomic hybridization. Cytometry 46: 222–232.

Chudoba I, Plesch A, Lorch T, Lemke J, Claussen U, Senger G. 1999. High resolution multicolor-banding: a new technique for refined FISH analysis of human chromosomes. Cytogenet Cell Genet 84:156–160.

Fauth C, Speicher MR. 2001. Classifying by colors: FISH-based genome analysis. Cytogenet Cell Genet 93:1–10.

Fauth C, Zhang H, Harabacz S, Brown J, Saracoglu K, Lederer G, Rittinger O, Rost I, Eils R, Kearney L, Speicher MR. 2001. A new strategy for the detection of subtelomeric rearrangements. Hum Genet 109:576–583.

Finelli P, Stanyon R, Plesker R, Ferguson-Smith MA, O'Brien PC, Wienberg J. 1999. Reciprocal chromosome painting shows that the great difference in diploid number between human and African green monkey is mostly due to non-Robertsonian fissions. Mamm Genome 10:713–718.

Fiegler H, Carr P, Douglas EJ, Burford DC, Hunt S, Scott CE, Smith J, Vetrie D, Gorman P, Tomlinson IP, Carter NP. 2003. DNA microarrays for comparative genomic hybridization based on DOP-PCR amplification of BAC and PAC clones. Genes Chromosomes Cancer 36:361–374.

Guan XY, Zhang H, Bittner M, Jiang Y, Meltzer P, Trent J. 1996. Chromosome arm painting probes. Nat Genet 12:10–11.

Harrison CJ, Foroni L. 2002. Cytogenetics and molecular genetics of acute lymphoblastic leukemia. Rev Clin Exp Hematol 6:91–113.

Henegariu O, Bray-Ward P, Ward DC. 2000. Custom fluorescent-

nucleotide synthesis as an alternative method for nucleic acid labeling. Nat Biotechnol 18:345–348.
Johnson JP, Demmer-Dieckmann M, Meo T, Hadam MR, Riethmuller G. 1981. Surface antigens of human melanoma cells defined by monoclonal antibodies. I. Biochemical characterization of two antigens found on cell lines and fresh tumors of diverse tissue origin. Eur J Immunol 11:825–831.
Leibovitz A, Stinson JC, McCombs WB, McCoy CE, Mazur KC, Mabry ND. 1976. Classification of human colorectal adenocarcinoma cell lines. Cancer Res 36:4562–4569.
Lengauer C, Speicher MR, Popp S, Jauch A, Taniwaki M, Nagaraja R, et al. 1993. Chromosomal bar codes produced by multicolor fluorescence in situ hybridization with multiple YAC clones and whole chromosome painting probes. Hum Mol Genet 2:505–512.
Liehr T, Weise A, Heller A, Starke H, Mrasek K, Kuechler A, Weier HU, Claussen U. 2002. Multicolor chromosome banding (MCB) with YAC/BAC-based probes and region-specific microdissection DNA libraries. Cytogenet Genome Res 97:43–50.
Melcher R, Steinlein C, Feichtinger W, Muller CR, Menzel T, Luhrs H, Scheppach W, Schmid M. 2000. Spectral karyotyping of the human colon cancer cell lines SW480 and SW620. Cytogenet Cell Genet 88:145–152.
Müller S, Rocchi M, Ferguson-Smith MA, Wienberg J. 1997. Toward a multicolor chromosome bar code for the entire human karyotype by fluorescence in situ hybridization. Hum Genet 100: 271–278.
Müller S, O'Brien PC, Ferguson-Smith, MA, Wienberg J. 1998. Cross-species colour segmenting: a novel tool in human karyotype analysis. Cytometry 33:445–452.
Müller S, Neusser M, O'Brien PC, Wienberg J. 2001. Molecular cytogenetic characterization of the EBV-producing cell line B95–8 (*Saguinus oedipus*, Platyrrhini) by chromosome sorting and painting. Chromosome Res 9:689–693.
Müller S, Neusser M, Wienberg J. 2002. Towards unlimited colors for fluorescence in-situ hybridization (FISH). Chromosome Res 10:223–232.
Ried T, Baldini A, Rand TC, Ward DC. 1992. Simultaneous visualization of seven different DNA probes by in situ hybridization using combinatorial fluorescence and digital imaging microscopy. Proc Natl Acad Sci USA 89:1388–1392.
Ried T, Schröck, E, Ning Y, Wienberg J. 1998. Chromosome painting: a useful art. Hum Mol Genet 7:1619–1626.
Roberts I, Wienberg J, Nacheva E, Grace C, Griffin D, Coleman N. 1999. Novel method for the production of multiple colour chromosome paints for use in karyotyping by fluorescence in situ hybridisation. Genes Chromosomes Cancer 25:241–250.
Saracoglu K, Brown J, Kearney L, Uhrig S, Azofeifa J, Fauth C, Speicher MR, Eils R. 2001. New concepts to improve resolution and sensitivity of molecular cytogenetic diagnostics by multicolor fluorescence in situ hybridization. Cytometry 44:7–15.
Schneider U, Schwenk HU, Bornkamm G. 1977. Characterization of EBV-genome negative "null" and "T" cell lines derived from children with acute lymphoblastic leukemia and leukemic transformed non-Hodgkin lymphoma. Int J Cancer 19:621–626.
Schröck E, Padilla-Nash H. 2000. Spectral karyotyping and multi color fluorescence in situ hybridization reveal new tumor-specific chromosome aberrations. Semin Hemat 37:334–347.
Schröck, E, du Manoir S, Veldman T, Schoell B, Wienberg J, Ferguson-Smith MA, Ning Y, Ledbetter DH, Bar-Am I, Soenksen D, Garini Y, Ried T. 1996. Multicolor spectral karyotyping of human chromosomes. Science 273: 494–497.
Schulten HJ, Gunawan B, Otto F, Hassmann R, Hallermann C, Noebel A, Fuzesi L. 2002. Cytogenetic characterization of complex karyotypes in seven established melanoma cell lines by multiplex fluorescence in situ hybridization and DAPI banding. Cancer Genet Cytogenet 133:134–141.
Speicher MR, Gwyn Ballard S, Ward, DC. 1996. Karyotyping human chromosomes by combinatorial multi-fluor FISH. Nat Genet 12: 368–375.
Telenius H, Pelmear AHP, Tunnacliffe A, Carter NP, Behmel A, Ferguson-Smith MA, Nordenskjold M, Pfragner R, Ponder BAJ. 1992. Cytogenetic analysis by chromosome painting using DOP-PCR amplified flow-sorted chromosomes. Genes Chromosomes Cancer 4:257–263.
Thompson FH, Emerson J, Olson S, Weinstein R, Leavitt SA, Leong SP, Emerson S, Trent JM, Nelson MA, Salmon SE, et al. 1995. Cytogenetics of 158 patients with regional or disseminated melanoma. Subset analysis of near-diploid and simple karyotypes. Cancer Genet Cytogenet 83:93–104.
Veldman T, Vignon C, Schröck E, Rowley JD, Ried T. 1997. Hidden chromosome abnormalities in haematological malignancies detected by multicolour spectral karyotyping. Nat Genet 15:406–410.
Wiegant J, Bezrookove,V, Rosenberg C, Tanke HJ, Raap AK, Zhang H, Bittner M, Trent JM, Meltzer P. 2000. Differentially painting human chromosome arms with combined binary ratio-labeling fluorescence in situ hybridization. Genome Res 10:861–865.
Wienberg J, Müller S. 2002. Chromosome bar codes: Defining karyotypes with molecular tags by multi color FISH. E.C.A. Newsletter 9:3–8.